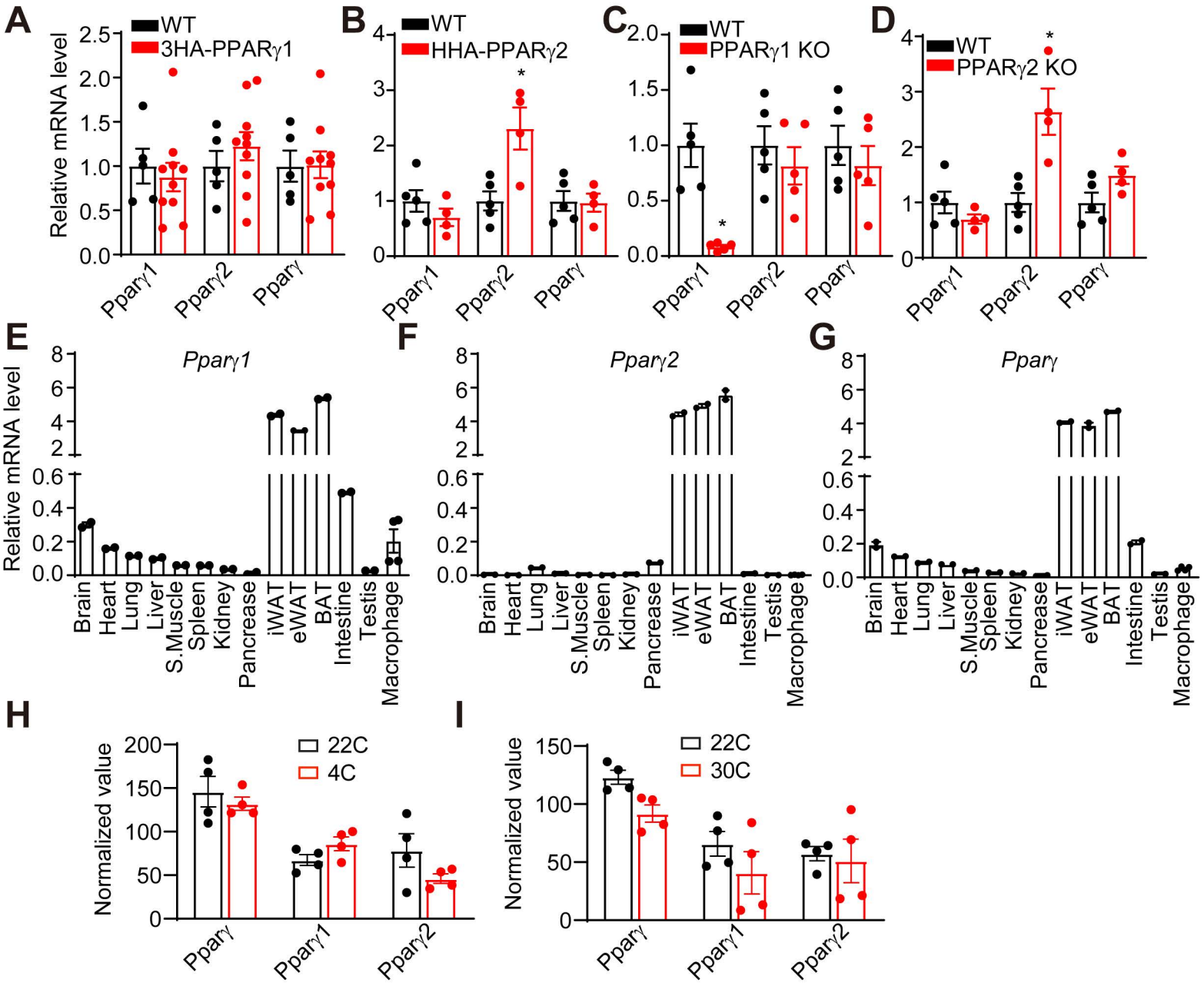

Figure S1. PPARγ1 and PPARγ2 expression levels in various mouse models. (A-D). mRNA expression of *PPARγ1, PPARγ2* and total *PPARγ* in iWAT of 3HA-PPARγ1 (A), HHA-PPARγ2 (B), PPARγ1 KO (C) and PPARγ2 KO mice (D) in iWAT, normalized to *Arbp*; WT was set to 1, as measured by qRT-PCR. n = 4-10 per group. **(E-G).** mRNA expression of *PPARγ1* (E), *PPARγ2* (F) and total *PPARγ* (G) in various tissues. n = 2-4 per group. Data are expressed as mean ± SEM. *p < 0.05 (Student's t test). **(H and I**). mRNA expression of total *PPARγ*, *PPARγ1 and PPARγ2* under 4 °C (H) and 30 °C (I). n = 4 per group. Data are expressed as mean ± SEM, as measured by RNA-seq.

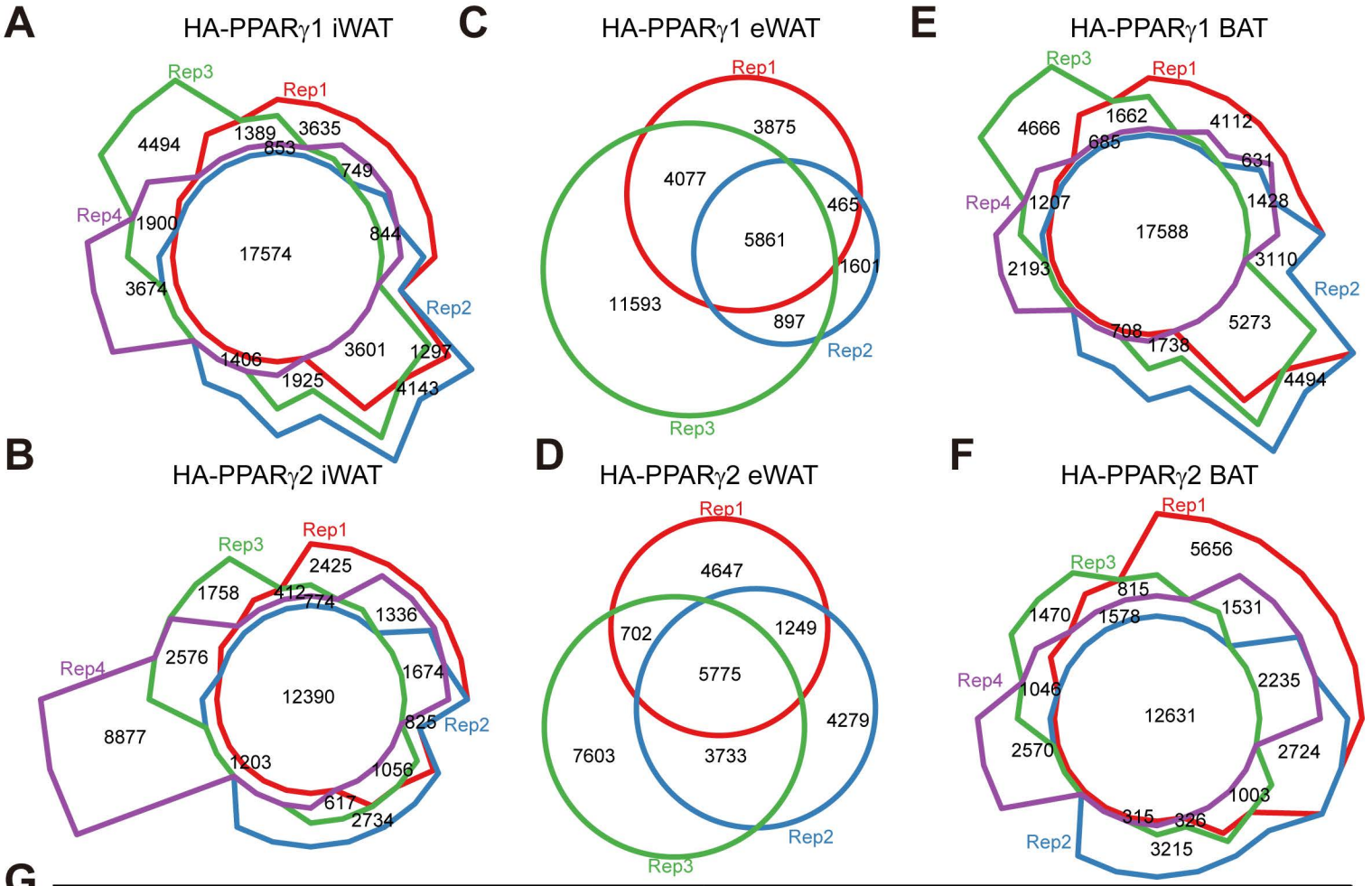

G

eWAT HA-PPARγ1 sites	Motif	P-value	%	eWAT HA-PPARγ2 sites	Motif	P-value	%
	PPARE	1e-1990	34.2		PPARE	1e-1485	33.9
	CEBPA	1e-844	30.2		CEBPA	1e-881	27.6
	NFI	1e-382	21.8		NFI	1e-412	40

BAT HA-PPARγ1 sites	Motif	P-value	%	BAT HA-PPARγ2 sites	Motif	P-value	%
	PPARE	1e-3250	36.5		PPARE	1e-2265	38.7
	CEBPA	1e-1943	28		CEBPA	1e-2039	33.6
	NFI	1e-1304	43.9		NFI	1e-949	53

H

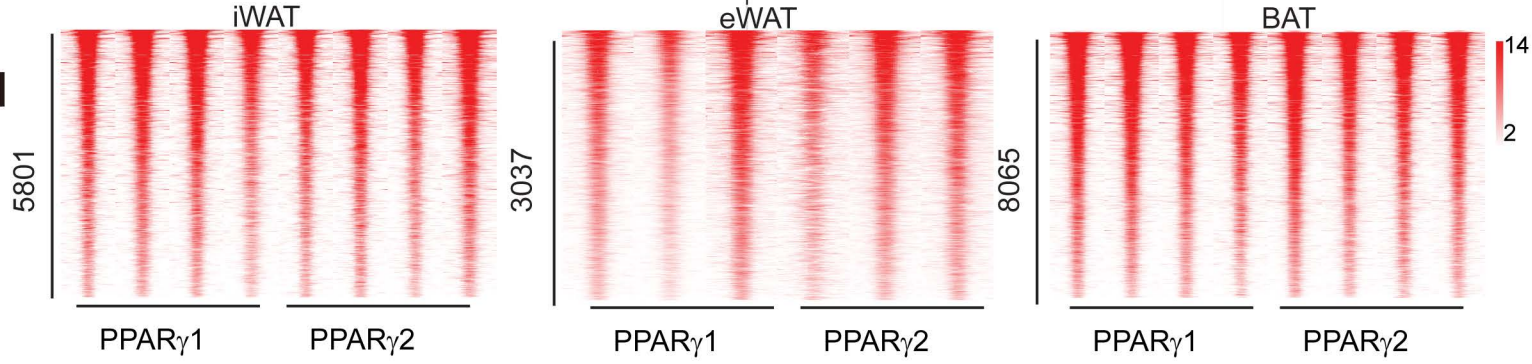

Figure S2. Characterization of the cistromes of PPARγ1 and PPARγ2. **(A-F).** Venn diagram showing the overlap of the cistromes of HA-PPARγ1 (A, C, and E) and HA-PPARγ2 from each biological replicate in three adipose depots (B, D, and F). **(G).** Top motifs enriched in PPARγ1 and PPARγ2 binding sites using Homer de novo motif analysis. **(H).** Heat map shows PPARγ1- or PPARγ2 common sites in three or four biological replicates from three adipose depots.

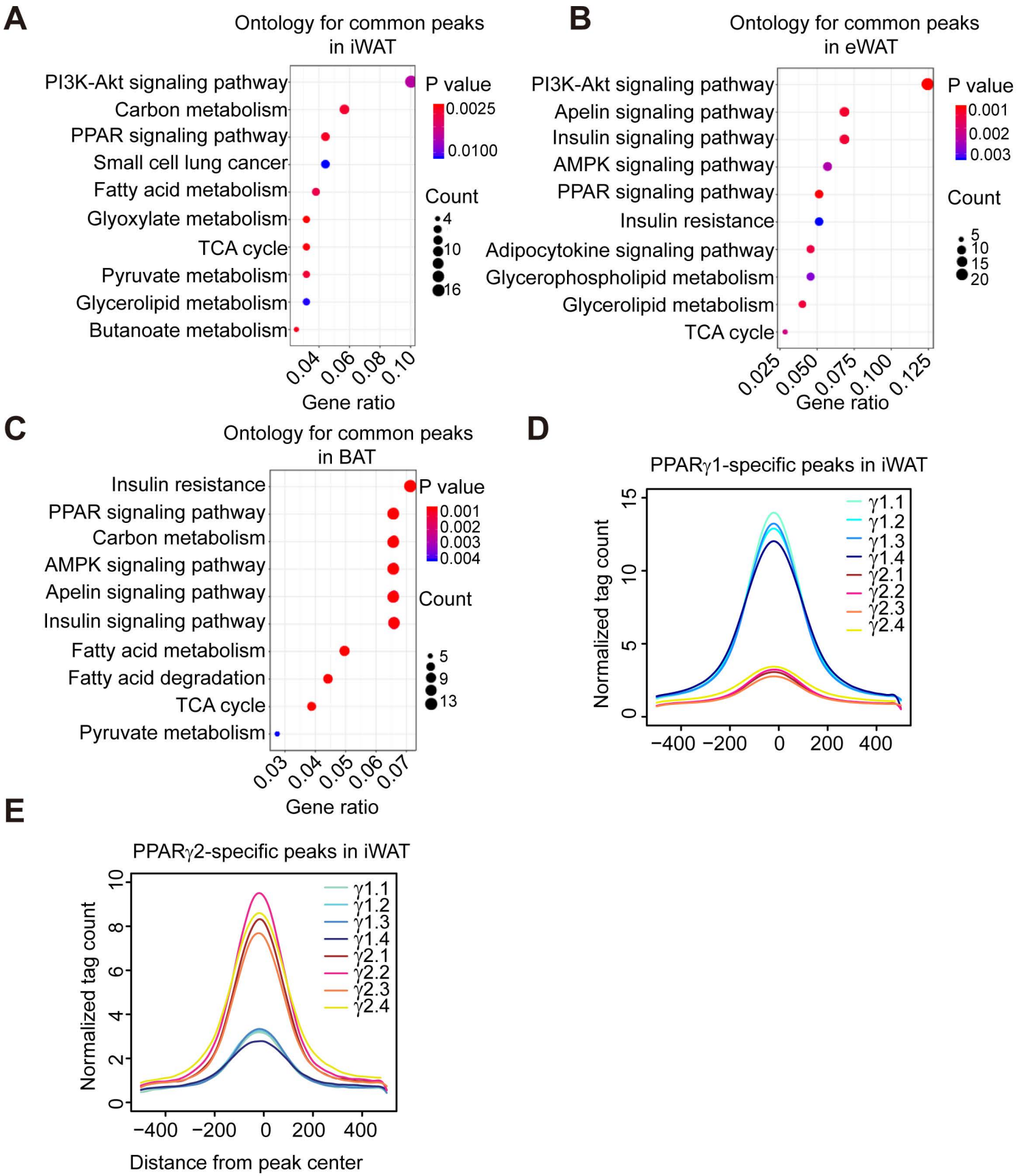

Figure S3. Annotation of PPARγ1- and PPARγ2-specific peaks. (A-C). Gene ontology for the nearest genes of common PPARγ binding sites that are detected similarly in PPARγ1 and PPARγ2 cistromes in iWAT (A), eWAT (B) and BAT (C). **(D).** For PPARγ1-specific peaks in iWAT, the average binding profiles are shown in 1 kb windows. **(E).** For PPARγ2-specific peaks in iWAT, the average binding profiles are shown in 1 kb windows.

A iWAT

Common sites	Motif	P-value	%
	PPARE	1e-990	52.0
	CEBP	1e-777	43.3
	NFI	1e-331	49.6

B eWAT

Common sites	Motif	P-value	%
	PPARE	1e-659	58.3
	CEBPA	1e-448	41.8
	NFI	1e-162	49.4

C BAT

Common sites	Motif	P-value	%
	CEBPA	1e-1353	43.5
	PPARE	1e-1213	44.1
	NFI	1e-574	65.1

D

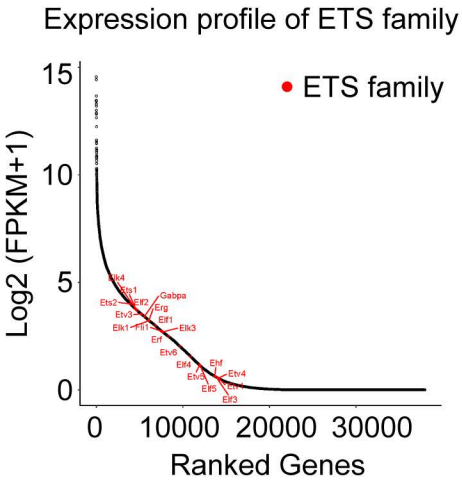

Figure S4. De novo motif analysis of common PPARγ binding sites in three adipose depots. (A-C). De novo motif analysis of common PPARγ binding sites in iWAT (A), eWAT (B) and BAT (C). **(D).** The expression profile of ETS family members in iWAT.

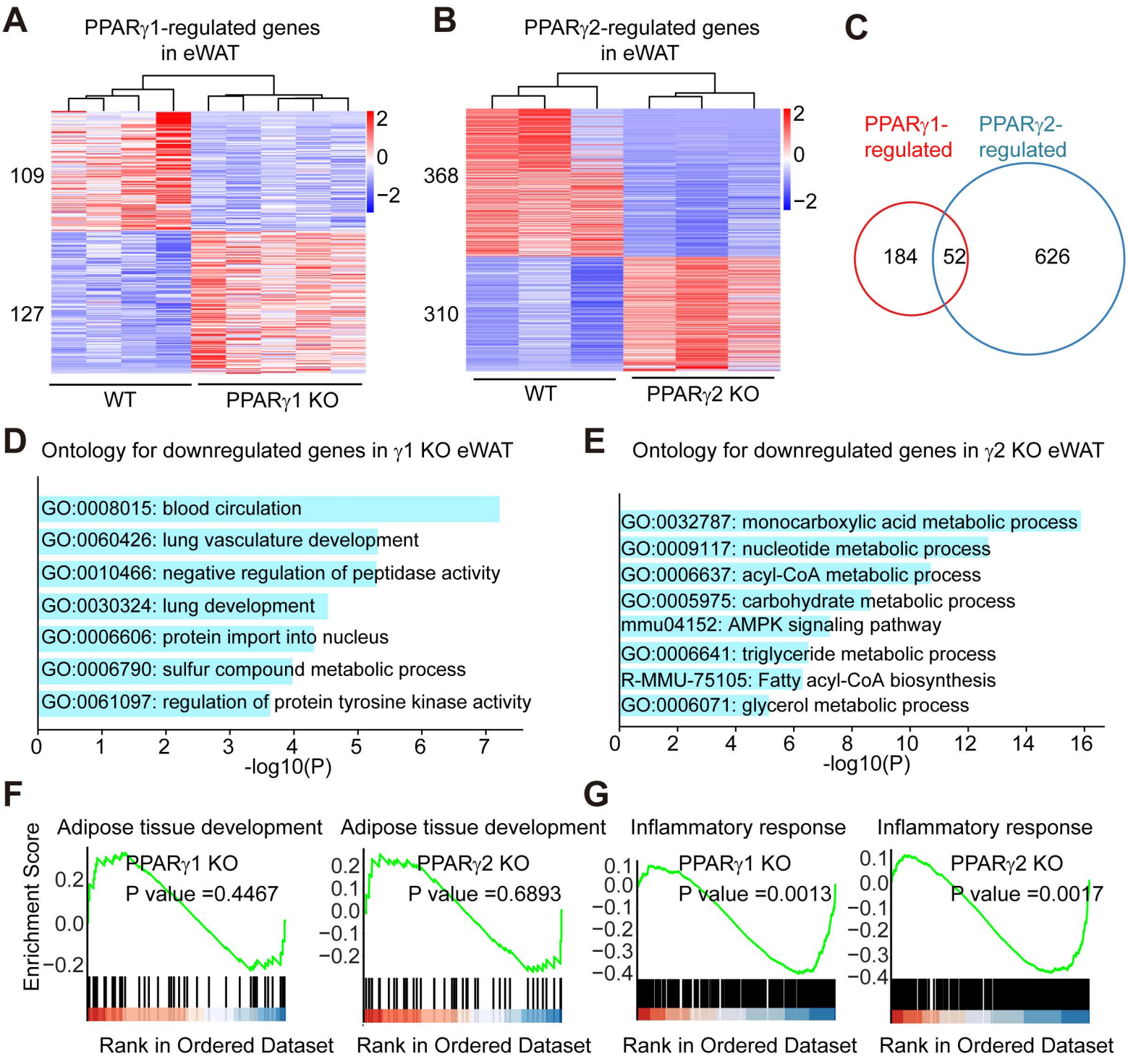

Figure S5. PPARγ1 and PPARγ2 regulate differential set of genes in eWAT. (A and B). Heatmap of the genes differentially expressed in PPARγ1 KO (A) and PPARγ2 KO mice (B) in eWAT. Three or four biological replicates, DE cutoff: |FC|> 1.5, FDR< 0.01. **(C).** Venn diagram showing the comparison of the PPARγ1- and PPARγ2-regulated genes in eWAT. **(D and E).** Gene ontology analysis of genes differentially expressed in PPARγ1 KO (D) and PPARγ2 KO mice (E). **(F and G).** GSEA analysis showing the no enrichment of adipose tissue development pathway for PPARγ1-regulated genes and PPARγ2-regulated genes (F), but significant enrichment of inflammatory response pathway for both PPARγ1-regulated genes and PPARγ2-regulated genes in BAT (G). Genes were ranked by average fold change in KO vs WT.

Wenxiang_sFig6

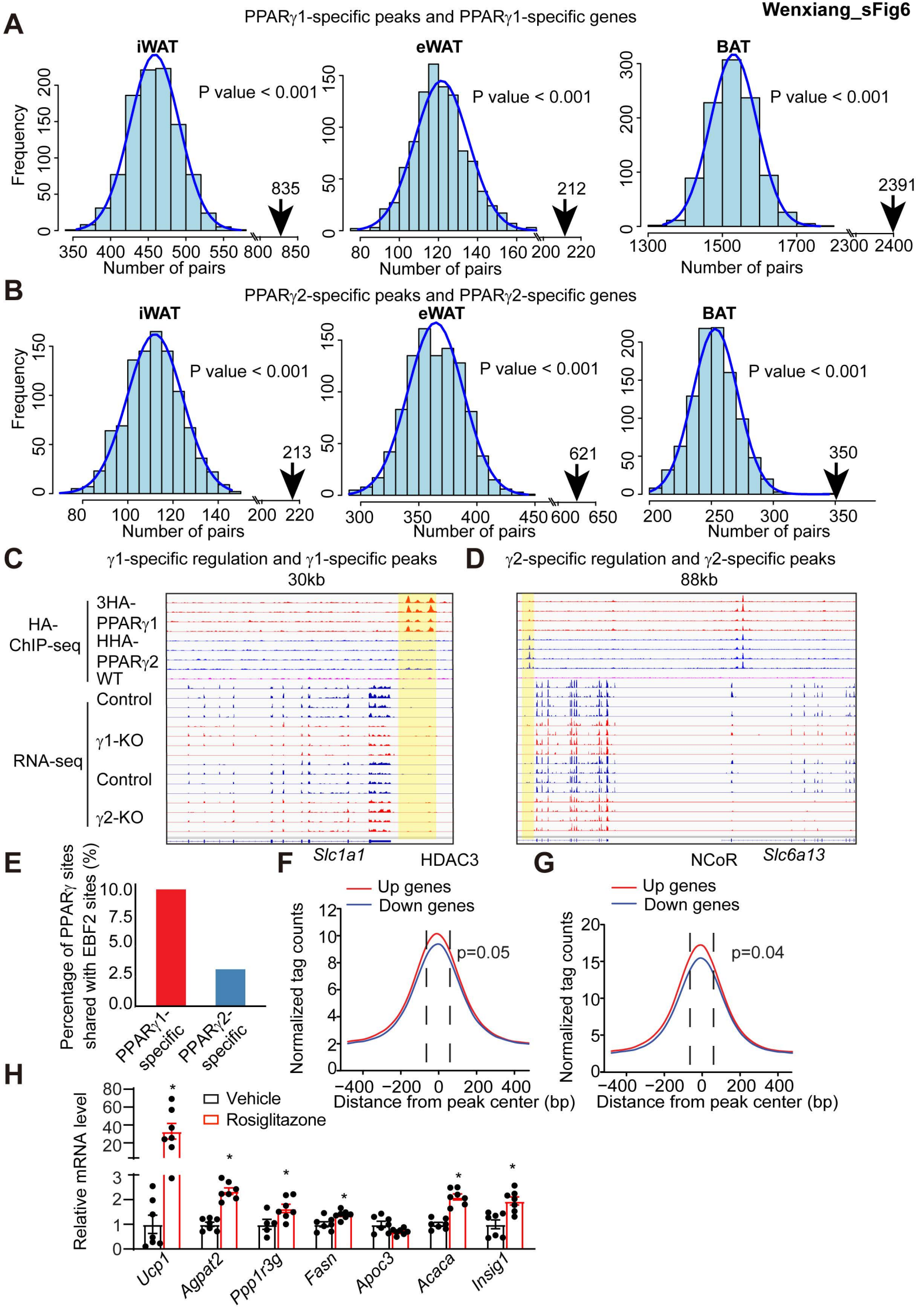

Figure S6. Differential genomic binding of PPARγ1 and PPARγ2 drives the differential regulation of genes. (A). PPARγ1-specific regulated genes are enriched in PPARγ1-specific peaks in iWAT, eWAT and BAT based on a permutation test. The pairs of PPARγ1-specific regulated genes that have PPARγ1-specific binding sites within 100 kb is indicated with a black arrow. The p values were calculated by permutation test. **(B).** PPARγ2-specific regulated genes are enriched in PPARγ2-specific peaks in iWAT, eWAT and BAT based on a random test. The pairs of PPARγ2-specific regulated genes that have PPARγ2-specific binding sites within 100 kb is indicated with a black arrow. The p values were calculated by permutation test. **(C and D).** Visualization of γ1-specifc binding (top) and γ1-specific gene regulation (bottom) at *Slc1a1* locus in 4 biological replicates (C), as well as γ2-specifc binding (top) and γ2-specific gene regulation (bottom) at *Slc6a13* locus (D). Yellow box indicates genomic regions with isoform-specific PPARγ binding. **(E).** Percentage of PPARγ1- and PPARγ2-specific binding sites shared with EBF2 binding sites. **(F and G).** The average peak intensities of HDAC3 (F) and NCoR (G) peaks overlapped with γ1-specifc peaks that associate with γ1-specifc regulated genes. *p < 0.05 (Student's t test). **(H).** mRNA expression of basally repressed genes by PPARγ1 in iWAT under rosiglitazone treatment, normalized to Arbp; Vehicle was set to 1, as measured by qRT-PCR. Data are expressed as mean ± SEM. *p < 0.05 (Student's t test).

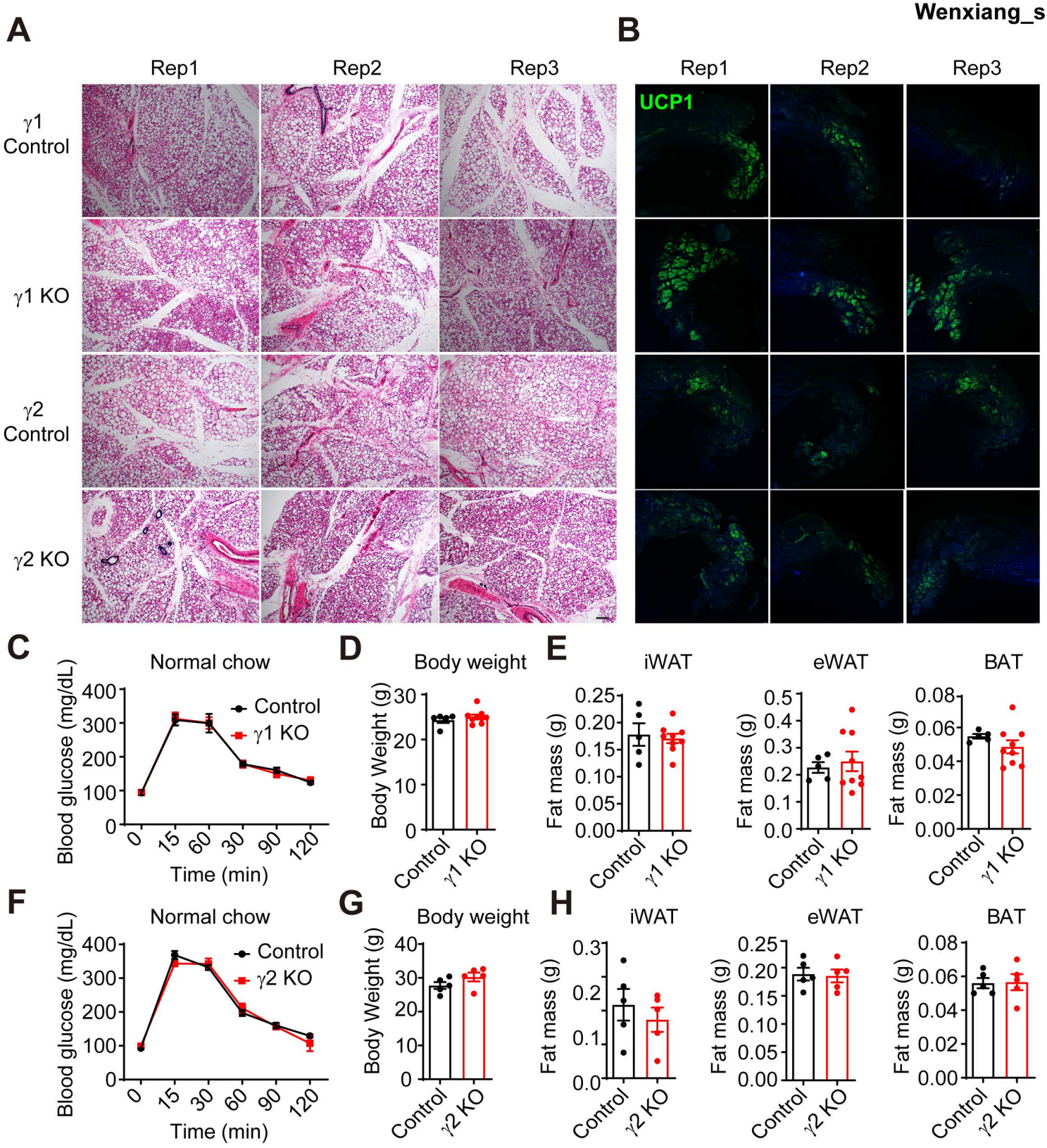

Figure S7. Normal metabolic phenotype of PPARγ1 KO and PPARγ2 KO mice on normal chow diet. (A and B). H&E staining (A) and Ucp1 staining (B) of iWAT from PPARγ1 KO and PPARγ2 KO mice and their control littermates housing at 4 °C for 5 days. n = 3 per group. Scale bar, 50 μm. **(C and F).** Intraperitoneal glucose tolerance test of PPARγ1 KO (C) and PPARγ2 KO mice (F) and their control littermates under normal chow diets. n = 4-9 per group. **(D and G).** Body weight of PPARγ1 KO (D) and PPARγ2 KO mice (G) and their control littermates on normal chow diet. n = 5-9 per group. **(E and H).** iWAT, eWAT and BAT weights from PPARγ1 KO (F) and PPARγ2 KO mice (H) and their control littermates on normal chow diet. n = 5-9 per group. Data are expressed as mean ± SEM.

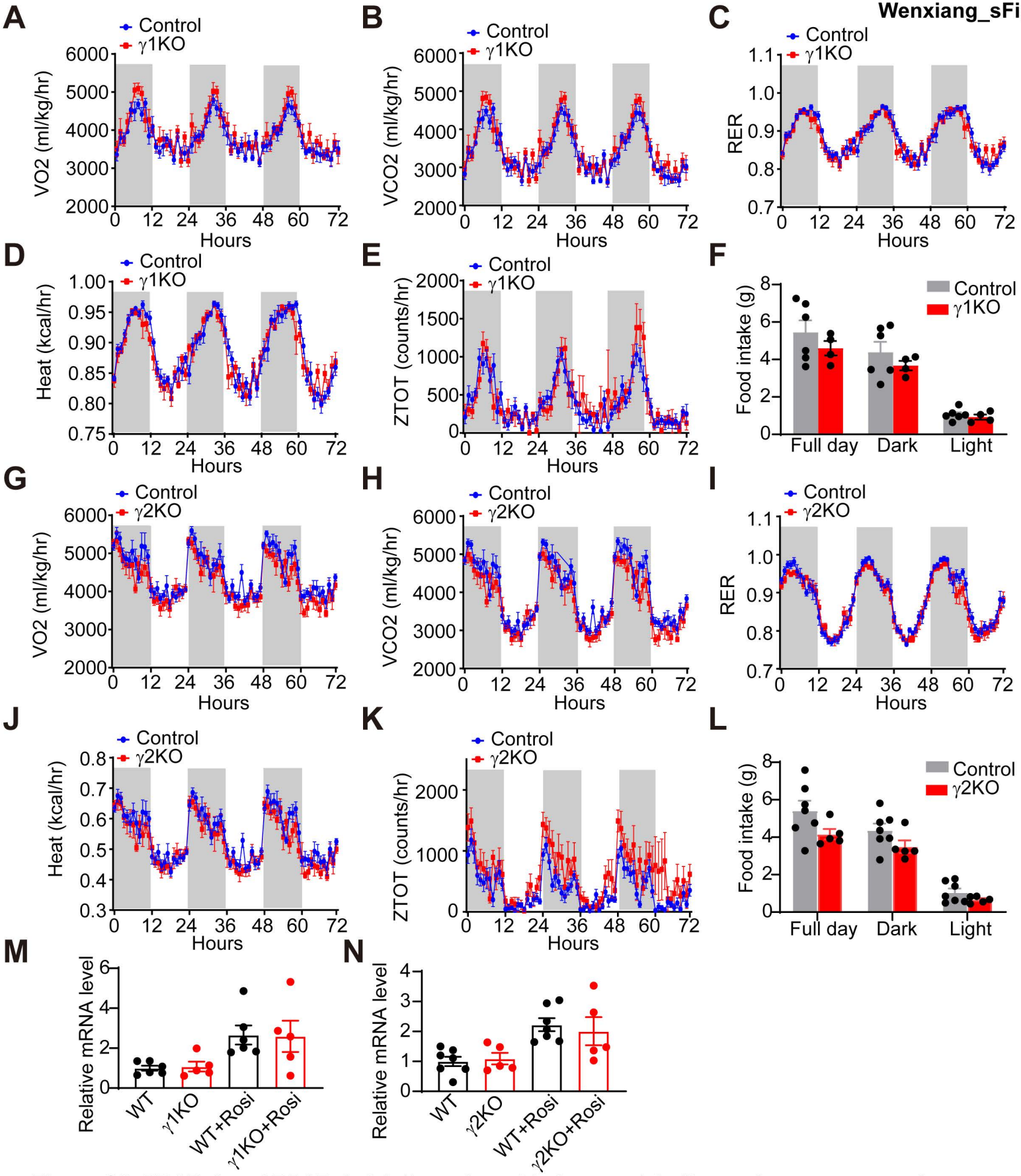

Figure S8. PPARγ1 and PPARγ2 deletions do not induce metabolic syndrome on normal chow diet. (A and G). Oxygen consumption (VO2) in PPARγ1 KO (A) and PPARγ2 KO mice (G) and their control littermates under NCD. **(B and H).** Carbon dioxide production (VCO2) in PPARγ1 KO (B) and PPARγ2 KO mice (H) and their control littermates on NCD. **(C and I).** Respiratory Exchange Ratio (RER) in PPARγ1 KO (C) and PPARγ2 KO mice (I) and their control littermates on NCD. **(D and J).** Heat production in PPARγ1 KO (D) and PPARγ2 KO mice (J) and their control littermates on NCD. **(E and K).** Locomotor activity of PPARγ1 KO (E) and PPARγ2 KO mice (K) and their control littermates on NCD. **(F and L).** Food intake of PPARγ1 KO (F) and PPARγ2 KO mice (L) and their control littermates on NCD. **(M and N).** mRNA expression of GK in PPARγ1 KO (M) and PPARγ2 KO mice (N) and their control littermates under rosiglitazone treatment, normalized to Arbp; WT mice was set to 1, as measured by qRT-PCR. Data are expressed as mean ± SEM.

Table S1. Primers used in this study.

Primer for RT-qPCR		
Primers	**Forward (5'-3')**	**Reverse (5'-3')**
Arbp	TCCAGGCTTTGGGCATCA	CTTTATCAGCTGCACATCACTCAGA
Pparγ1	AGAAGCGGTGAACCACTGATATTC	AGAGGTCCACAGAGCTGATTCC
Pparγ2	TGGGTGAAACTCTGGGAGATTC	GAGAGGTCCACAGAGCTGATTCC
Pparγ	GACCTGAAGCTCCAAGAATACC	ACAGACTCGGCACTCAATG
Ucp1	TCAGGATTGGCCTCTACGAC	TGCCACACCTCCAGTCATTA
GK	CGGAGACCAGCCGTGTTAAG	GTCCACTGCTCCCACCAATG
Agpat2	CAGCCAGGTTCTACGCCAAG	TGATGCTCATGTTATCCACGGT
Ppp1r3g	TGGCAACGATGCCTGATCC	CCACTCCGTGAAAGTGTAGC
Fasn	TACAGGAGTTCTGGGCCAAC	GACCGCTTGGGTAATCCATA
Apoc3	TACAGGGCTACATGGAACAAGC	CAGGGATCTGAAGTGATTGTCC
Acaca	CTTCCTGACAAACGAGTCTGG	CTGCCGAAACATCTCTGGGA
Insig1	CACGACCACGTCTGGAACTAT	TGAGAAGAGCACTAGGCTCCG